Available online at www.sciencedirect.com

SciVerse ScienceDirect

Ceramics International 38 (2012) 4271–4276

CERAMICS INTERNATIONAL

www.elsevier.com/locate/ceramint

Synthesis and microwave dielectric properties of pseudobrookite-type structure $Mg_5Nb_4O_{15}$ ceramics by aqueous sol–gel technique

H.T. Wu *, W.B. Wu, Y.L. Yue, Y.M. Chen, F. Yang

Shandong Provincial Key Laboratory of Preparation and Measurement of Building Materials, University of Jinan, Jinan 250022, China

Received 7 January 2012; received in revised form 25 January 2012; accepted 31 January 2012
Available online 18 February 2012

Abstract

Pseudobrookite-type $Mg_5Nb_4O_{15}$ ceramics were prepared by aqueous sol–gel process and microwave dielectric properties were investigated. Highly reactive nanosized $Mg_5Nb_4O_{15}$ powders were successfully synthesized at 600 °C in oxygen atmosphere with particle sizes of 20–40 nm firstly and then phase evolution was detected by DTA-TG and XRD. Sintering characteristics and microwave dielectric properties of $Mg_5Nb_4O_{15}$ ceramics were studied at different temperatures ranging from 1200 °C to 1400 °C. With the increase of sintering temperature, density, ε_r and $Q{\cdot}f$ values increased, and then saturated at 1300 °C. Excellent microwave properties of ε_r ~11.3, $Q{\cdot}f$ ~43,300 GHz and τ_f ~−58 ppm/°C, were obtained finally. The sintering temperature of $Mg_5Nb_4O_{15}$ ceramics was significantly reduced by aqueous sol–gel process compared to conventional solid-state methods.

Keywords: A. Sol–gel processes; $Mg_5Nb_4O_{15}$; Nanopowder synthesis; Microwave dielectric properties

1. Introduction

The rapid progress in mobile and satellite communication system were creating high demands for the development of microwave dielectric materials with a high quality factor, an appropriate dielectric constant, and a near-zero temperature coefficient of resonant frequency. $A_5B_4O_{15}$ (A = Ba, Sr, Mg, Ca; B = Nb, Ta) dielectric ceramics were investigated and had good microwave dielectric properties [1]. Among them, $Mg_5Nb_4O_{15}$ (MN) compound was investigated with the isostructural structure of pseudobrookite Fe_2TiO_5 [2] and its space group was orthorhombic $D_{2h}{}^{17}$-*cmcm* with $Z = 4$. The structure consisted of double chains of $(Mg,Nb)O_6$ units, sharing edges of the *bc* plane, interconnected through common oxygen along the *a* axis to give a three-dimensional array. Sebastian et al. reported that microwave properties of $Mg_5Nb_4O_{15}$ compounds sintered at 1450 °C were ε_r ~11, $Q{\cdot}f$ ~37,400 GHz by solid state process [1]. Kamba et al. also reported that $Mg_5Nb_4O_{15}$ compounds were sintered at 1450 °C with microwave properties of ε_r ~11, $Q{\cdot}f$ ~37,350 GHz, and τ_f ~−54 ppm/°C by solid-state process[3]. Obviously high sintering temperatures would limit their applications for practical cases, so the reduction of sintering temperature was desirable to enable commercial applications. Usually it was believed that lowering sintering temperatures could be achieved by many methods such as chemical processing, adding glass flux, and using starting materials with smaller particle sizes, and so on. It was well known that adding glass flux usually caused detrimental effect on microwave properties. Now in order to reduce sintering temperatures and improve sintering ability there were many other investigations of chemical processing (i.e. coprecipitation, sol–gel process, hydrothermal method, etc.), which had been developed as alternatives to the conventional solid-state reaction of mixed oxides for producing ceramics by using starting materials with smaller particle sizes. Among of these methods, the sol–gel process was undoubtedly one of useful methods for producing powders with good control over stoichiometry and homogeneity, yielding nano-sized particles and widely used in many other ceramics system [4–8]. However, few researches about microwave properties of MN ceramics fabricated by sol–gel process were reported in present literatures.

The goal of this research was to explore capabilities of sol–gel method to synthesize nano-sized powders as precursors for the preparation of MN ceramics promisingly sintered at low

* Corresponding author.
E-mail address: mse_wuht@ujn.edu.cn (H.T. Wu).

0272-8842/$36.00
doi:10.1016/j.ceramint.2012.01.084

temperatures. The whole process involved all complexation of aqueous metal ions by non-toxic poly functional carboxyl and avoided complex steps such as refluxing of alkoxides, resulting in less time consumption compared to other techniques. Phase formation originated from the gel and microwave dielectric properties of MN ceramics as a function of sintering temperatures were investigated in detail. Experimental results showed that the aqueous sol–gel process was the most effective and least expensive technique used for the preparation of MN ceramics with retaining excellent microwave properties at low sintering temperatures.

2. Experimental

Analytical-grade Nb_2O_5, K_2CO_3, $Mg(NO_3)\cdot 6H_2O$, HNO_3, citric acid (CA) and ethylene glycol (EG) were used as raw materials to synthesize MN nanopowders as shown in Fig. 1. Firstly, the mixture of Nb_2O_5 and K_2CO_3 with the ratio of 1:4 was co-melted at 900 °C in order to obtain K_3NbO_4 compounds according to phase diagrams. Subsequently, K_3NbO_4 compounds were dissolved in distilled water, then pH value was controlled at ~2 to ensure the formation of $Nb(OH)_5$ precipitate. The whole formation process of $Nb(OH)_5$ precipitate could be formulated as shown in Eqs. (1)–(4). Thirdly, $Nb(OH)_5$ precipitate was filtered off and washed with distilled water for six times to remove the K^+ ions and then dissolved completely in citric acid water solution by continuous magnetic stirring at 300 rpm for 15 min. Meanwhile, a stoichiometric amount of $Mg(NO_3)\cdot 6H_2O$ was added to the above solution and then the solution was stirred for another 30 min. Finally, the ethyl alcohol (20–40 ml) was added to the as-prepared mixed solution in drops and stirred for 1 h to obtain transparent and stable sol. pH value was maintained in the range of 3.5–5 by adding buffering agents. The sol was heated at 80–90 °C for 5 h to obtain a xerogel. The xerogel was decomposed at 600 °C using a muffle furnace for crystallization in oxygen atmosphere. As-prepared powers were ball milled in a polyethylene jar for 4 h using ZrO_2 balls in ethanol medium to reduce the conglobation phenomena. After drying, the powder was then mixed with polyvinyl alcohol as a binder, granulated and pressed into cylindrical disks of 10 mm diameter and about 5 mm height at a pressure of about 200 MPa. These pellets were preheated at 600 °C for 4 h to expel the binder and then sintered at selected temperatures for 2 h in air at a heating rate of 5 °C/min.

$$3K_2CO_3 + Nb_2O_5 \rightarrow 2K_3NbO_4 + CO_2. \quad (1)$$

$$6K_3NbO_4 + 5H_2O \rightarrow 18K^+ + Nb_6O_{19}^{8-} + 10OH^-. \quad (2)$$

$$4K^+ + Nb_6O_{19}^{8-} + 4OH^- + 8H^+ \rightarrow K_4H_4Nb_6O_{19}\downarrow + 4H_2O. \quad (3)$$

$$K_4H_4Nb_6O_{19} + 15H^+ + 11OH^- \rightarrow 6Nb(OH)_5\downarrow + 4K^+. \quad (4)$$

In order to analyze the evolution of MN phase formation, the as-prepared xerogel was characterized using thermogravimetry (TG) and differential thermal analysis (DTA) to study thermal properties. Phase analysis was conducted with the help of a Rigaku diffractometer (Model D/MAX-B, Rigaku Co., Japan) using Ni filtered Cu Kα radiation (λ = 0.1542 nm) at 40 kV and 40 mA settings. Based on XRD analysis, raw MN powders were examined for morphology and particle size using a transmission electron microscopy (Model JEOL JEM-2010, FEI Co., Japan). Bulk densities of sintered ceramics were measured by the Archimedes method. An HP8720ES network analyzer (Hewlett-Packard, Santa Rosa, CA) was used for the measurement of microwave dielectric properties. The dielectric constant was measured using Hakki–Coleman post-resonator method by exciting TE011 resonant modes of dielectric resonators as suggested by Hakki and Coleman and Courtney [9]. Unloaded quality factors were measured using the TE01d mode by a cavity method [10]. All measurements were made at room temperature and in the frequency of 8–10 GHz. The temperature coefficient of resonant frequency was measured in the temperature range of 25–85 °C.

3. Results and discussion

Fig. 2 showed TG-DTA curves of MN xerogel in pure oxygen atmosphere at a heating rate of 10 °C/min. It was found

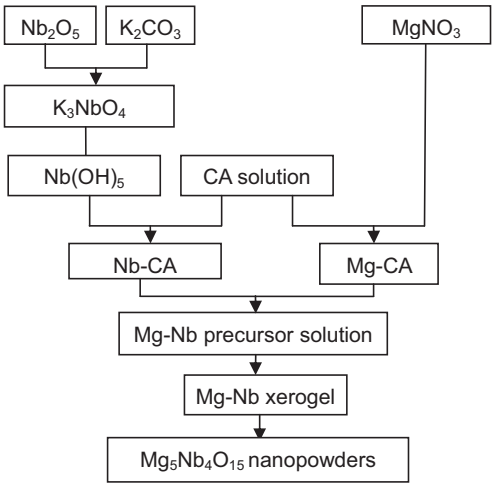

Fig. 1. Chart for synthesis of MN nanopowders by aqueous sol–gel process.

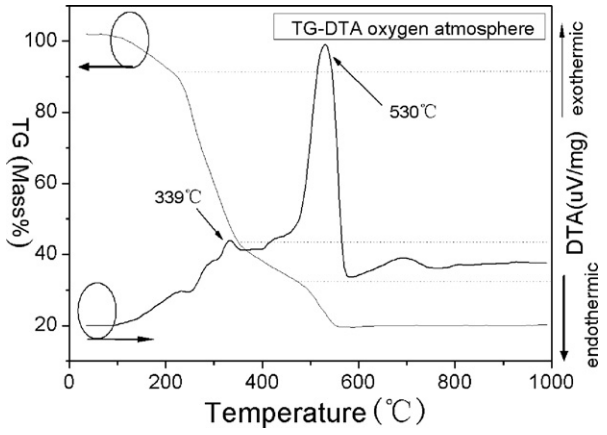

Fig. 2. TG-DTA curves of MN xerogel in oxygen atmosphere.

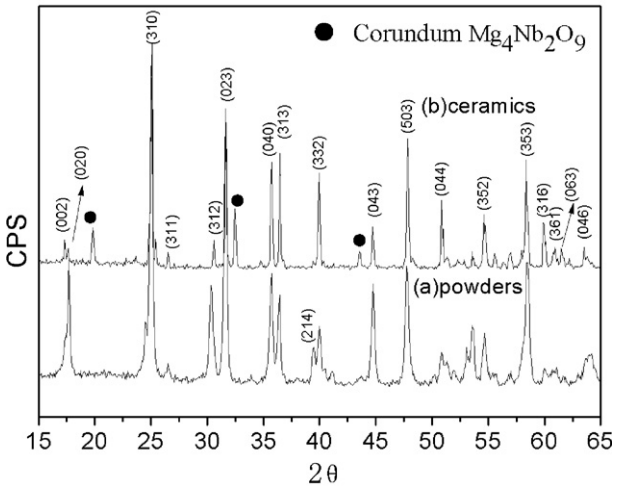

Fig. 3. X-ray diffraction patterns of MN xerogel calcined at (a) 600 °C for 30 min and ceramics sintered at 1300 °C for 2 h.

that obvious weight loss began at 80 °C and all chemical reactions involving weight losses, such as decomposition of organic polymeric networks with evolution of CO_2 and H_2O, were completed below 600 °C. Total weight loss was about 80%, which occurred in three steps: (i) initial weight loss (about 10%) below 250 °C, resulting from the evaporation of residual solvent and water, with wide and weak endothermic peaks, (ii) subsequent significant weight loss (about 60%) caused by decomposition of organic polymeric networks with evolution of CO_2 and H_2O, and (iii) final weight loss (about 10–20%) in TG curves, combined with an obviously exothermal peak in the temperature region of 500–600 °C, which was attributed to the oxidation of metal–organic groups. No further significant weight loss and thermometric peaks were observed above 600 °C in TG-DTA curves, indicating the minimum firing temperature to synthesize magnesium niobate compounds.

The XRD pattern of MN xerogel calcined at 600 °C for 30 min in oxygen atmosphere was shown in Fig. 3(a). It was pleasantly found that the crystallization of MN phase took place obviously at 600 °C, this kind of phenomenon was also recognized from exothermic peaks of DTA and corresponding TG profiles as described above. The xerogel fired at 600 °C consisted of predominant peaks of $Mg_5Nb_4O_{15}$ matching with JCPDS file number 20-0681, also free from any second phases such as $Mg_4Nb_2O_9$ or $MgNb_2O_6$. All reflections in diffraction patterns could be indexed on the basis of an orthorhombic phase with refined lattice parameters of a ~11.427 Å, b ~10.058 Å and c ~10.26 Å. In Fig. 3(a) the influence of calcination temperatures on X-ray diffraction of powders was observed in the variation of intensity and full width at half maximum (FWHM), characteristic peaks of (3 1 0) and (0 2 3) were narrower and stronger, which was associated with the crystallization of powders. According to the Scherer formula ($D = K\lambda/\beta \cos\theta$) [11], particle size of MN powders at 600 °C was calculated to be 32 nm. XRD results indicated that calcination temperature of synthesizing pure MN phase was remarkably reduced to 600 °C by aqueous sol–gel method, which showed obvious advantage over these of conventional mixed oxide routes reported before [1,3] as shown in Table 1. To be contrast, as-prepared MN ceramics sintered at different temperatures ranging from 1200 °C to 1400 °C also showed similar XRD patterns with sharper peaks and the representative pattern was demonstrated as shown in Fig. 3(b), which indicated that the $Mg_5Nb_4O_{15}$ compound existed as predominant phase in a status of excellent crystallization just with minor second phase of $Mg_4Nb_2O_9$.

The TEM micrograph of MN nanopowders calcined at 600 °C was illustrated in Fig. 4. As observed in the image, it was worth noting that particles were slightly agglomerated due to high surface to volume ratio and basically regular in shape. Particle sizes were measured by the liner intercept method [12] with the range of about 20–40 nm, which was in good coincidence with calculated results of Scherer formula mentioned above. Therefore MN powders had smaller particle size of 20–40 nm by aqueous sol–gel process with larger surface area and free energy. Since the surface free energy is considered to be a driving force during sintering process, a number of sintering models have been researched for initial sintering stages and the resulting equation has been deduced as formulated in Eq. (5). According to sintering equation of initial stages [13], the use of MN nanopowders as starting materials was effective in preparing MN ceramics with full density promisingly through low sintering temperature and short sintering time. Therefore, the sol–gel process showed significant advantages of sintering ceramics at relatively low temperatures theoretically.

$$\frac{\Delta L}{L_0} = \frac{K_1 D \gamma_s \Omega w}{G^m kT} t^n \tag{5}$$

where K_1 and w are constant, D is the diffusivity, γ_s is the surface energy, Ω is the atomic volume, G is the particle or grain size, k is the Boltzmann's constant, T is temperature, t is sintering time and m is a constant depending on diffusion paths.

The sintering characteristic of samples depending on sintering temperatures was plotted as shown in Fig. 5. Fig. 5 represented curves of apparent densities and diametric shrinkage ratio as a function of sintering temperatures, through

Table 1
Comparison of $Mg_5Nb_4O_{15}$ ceramics prepared by different methods.

Process	Calcination temperature (°C)	Sintering temperature (°C)	ρ (g/cm^3)	ε_r	$Q{\cdot}f$ (GHz)	τ_f (ppm/°C)	References
Solid-state	1300	1450	3.90	11	37,400	−54	[1]
Solid-state	–	1450	3.90	11	37,350	−54	[3]
Sol–gel	600	1300	3.87	11.3	43,300	−58	Our results

"–" denoted that no values were mentioned.

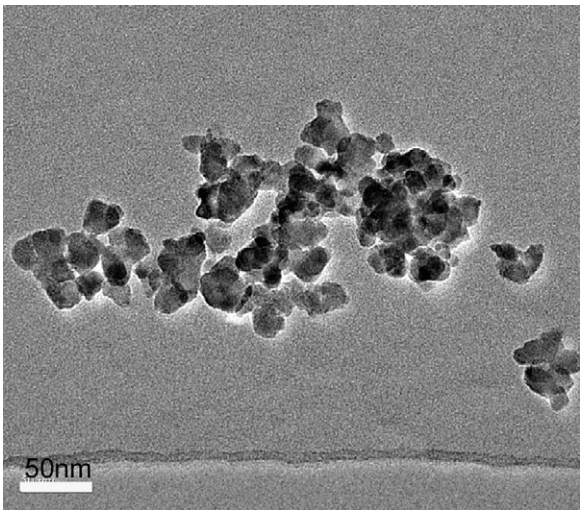

Fig. 4. TEM micrograph of raw MN nanopowders calcined at 600 °C for 30 min.

which the optimized sintering temperature was determined. Apparent densities increased from ~2.6 to ~3.9 g/cm^3 as sintering temperatures increased from 1200 °C to 1400 °C. A saturated value of apparent density was obtained at 1300 °C. The curve of diametric shrinkage ratio also showed the similar tendency with the increase of sintering temperature, and also saturated at about 1300 °C. SEM micrographs of MN ceramics sintered at different temperatures for 2 h were illustrated in Fig. 6(a)–(e). Changes in the porosity and grain size could be seen with the increase of sintering temperature. The apparent porosity decreased as sintering temperatures increased from 1200 °C to 1300 °C and all pores almost disappeared at 1300 °C on the surface of MN samples. As the sintering temperature increased, grains grew up rapidly and grain size measured by a linear intercept method [12] was about ~3 μm at 1300 °C as shown in Fig. 6(c). Moreover, the grain morphology of MN ceramics exhibited two types of grains: large grains and small cubic-shape grains dispersed on the surface of large grains. The concentration of Mg and Nb ions in large grains was analyzed to be 43.81 and 32.22 at.%, respectively. The ratio of Mg/Nb was approximately corresponding to $Mg_5Nb_4O_{15}$ phase. On the contrast, the concentration of Mg and Nb ions in small grains was analyzed to be 34.27 and 20.01 at.%, respectively. The ratio of Mg/Nb was approximately corresponding to $Mg_4Nb_2O_9$ phase. These analyses were in good agreement with XRD results as shown in Fig. 3(b). Based on above results, it was shown that MN ceramics were successfully prepared with high density through sol–gel process at 1300 °C and the sintering temperature was reduced significantly compared to solid-state reaction methods [1,3].

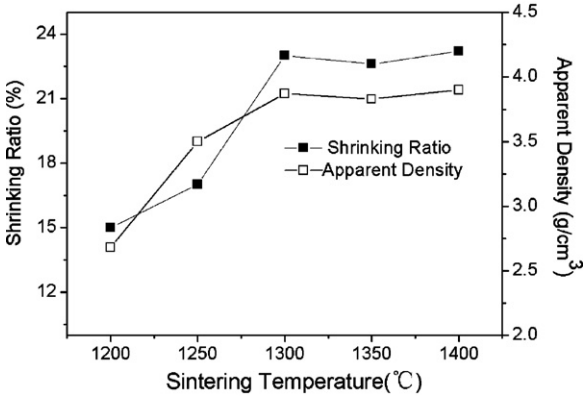

Fig. 5. Curves of apparent densities and shrinkaging ratio of MN ceramics as a function of sintering temperatures.

The plots of ε_r, $Q{\cdot}f$ and τ_f values were shown in Fig. 7 as a function of sintering temperatures. The ε_r value of MN ceramics steadily increased from 6.8 to 11.3 as sintering temperatures ranged from 1200 °C to 1300 °C, then saturated at ~11. Based on the result of microstructure as shown in Fig. 6, it was obvious that low ε_r values were caused by loosened microstructure with much pores at sintering temperatures <1300 °C. ε_r values were approximately saturated at ~11 when sintering temperatures >1300 °C. The curve of ε_r value showed a similar tendency with those of apparent density and shrinkage ratio, which were sensitive to dense degree of ceramics significantly. In general, higher density could achieve higher dielectric constant owing to a lower amount of pores ($\varepsilon_r \sim 1$). The result of ε_r value obtained at 1300 °C by sol–gel process was comparable with these of samples sintered at 1450 °C by solid-state reaction methods [1,3]. In addition, extra effect on dielectric constant caused by second phase of $Mg_4Nb_2O_9$ could be negligible due to its minor quantity and approximate dielectric constant ($\varepsilon_r \sim 12$) reported by Ogawa et al. [14] and Khalam et al. [15]. Moreover, to clarify the accuracy of experimental results and effect of crystal structure on the dielectric constant, theoretical dielectric polarizability ($\alpha_{\text{theo.}}$) was calculated to be ~58.84 by the additive rule with ionic polarizability of composing ions or oxides [16] as formulated in Eq. (6) and observed dielectric polarizability ($\alpha_{\text{obs.}}$) was calculated to be 58.5 by Clauses–Mosotti equation as formulated in Eq. (7) with measured dielectric constant at microwave frequencies [17]. Values of $\alpha_{\text{theo.}}$ and $\alpha_{\text{obs.}}$ were in good agreement with each other and minor deviation between them could attribute to effect of relative density and second phase because the $\alpha_{\text{obs.}}$ value depended on specimens and fabrication process.

$$\alpha_{\text{theo.}} = \alpha(Mg_5Nb_4O_{15}) = 5\alpha(MgO) + 2\alpha(Nb_2O_5) \quad (6)$$

$$\alpha_{\text{obs.}} = \frac{1}{b}\left[\frac{Vm(\varepsilon - 1)}{(\varepsilon + 1)}\right] \quad (7)$$

where $\alpha_{(MgO)}$ and $\alpha_{(Nb_2O_5)}$ represented oxides polarizabilities reported by Shannon [16]. Moreover, Vm, ε and b indicated the molar volume of unit cell, dielectric constant and constant value ($4\pi/3$), respectively.

With the increase of sintering temperatures from 1200 °C to 1300 °C, $Q{\cdot}f$ values increased from 18,954 GHz to 43,300 GHz with a saturated $Q{\cdot}f$ value ~43,000 GHz in the sintering temperature region of 1300–1400 °C. The remarkable increase in $Q{\cdot}f$ values ranging from 1200 °C to 1300 °C was also related to the reduction of porosity according to results of SEM microstructure as shown in Fig. 6(a)–(c). As for $Q{\cdot}f$ values, it

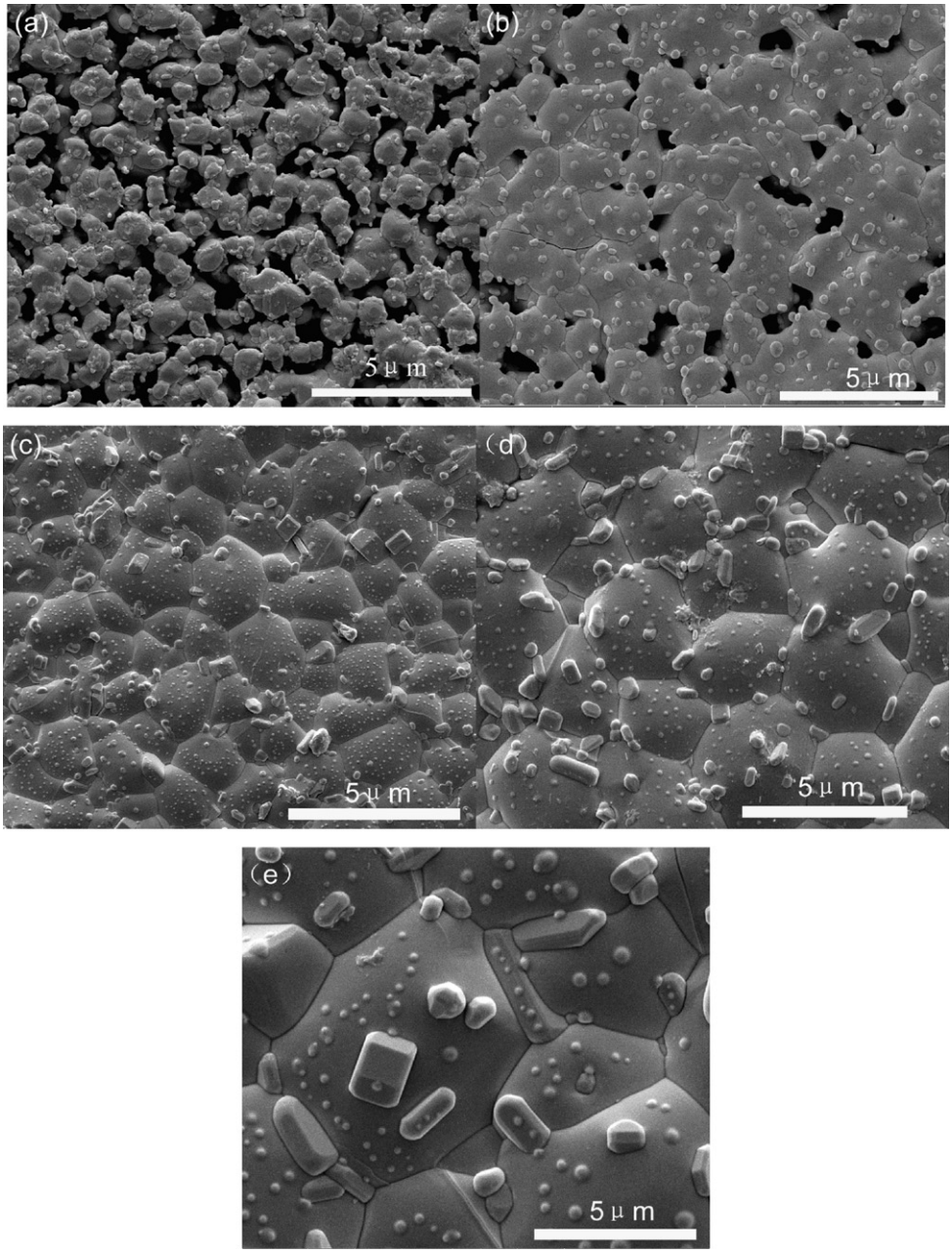

Fig. 6. FE-SEM micrographs of MN ceramics sintered at different sintering temperatures for 2 h ((a)–(e) corresponding to 1200 °C, 1250 °C, 1300 °C, 1350 °C, and 1400 °C).

was known that porosity, secondary phase, structure defect and grain boundary of ceramics as extrinsic factors usually produced a deterioration in $Q{\cdot}f$ values [18]. Among of these factors, on the one hand, porosity was suggested to affect $Q{\cdot}f$ values obviously at sintering temperatures less than 1300 °C associated with our results. Relative density was one of important factors in controlling dielectric loss, which had been verified on many other microwave dielectric materials. Due to the increased density MN ceramics sintered at 1300 °C had an excellent $Q{\cdot}f$ value of 43,300 GHz, which was higher than these of samples ($Q{\cdot}f \sim$ 37,400 GHz) sintered at 1475 °C by solid-state methods [1,3]. On the other hand, when as-prepared samples were of nearly full density, $Q{\cdot}f$ values were mainly affected by the second phase. As for $Mg_4Nb_2O_9$ phase, the crystal structure was investigated early with corundum structure by Sreedhar and Pavaskar [19]. Khalam et al. [15] reported a $Q{\cdot}f$ value of 116,000 GHz, then Fu et al. [20] reported a better $Q{\cdot}f$ value of 175,000 by high-energy ball-milling method, while Kan et al. [14] reported a relatively higher $Q{\cdot}f$ value of 193,000. According to well-known general empirical models for multiphase ceramics [21], the presence of $Mg_4Nb_2O_9$ phase would have significantly beneficial effect on $Q{\cdot}f$ values to some degree. Moreover, the remarkable variation in τ_f values was not recognized with sintering temperatures from 1200 °C to 1400 °C and these values were ranged from −50 to −60 ppm/°C. Similarly, the minor $Mg_4Nb_2O_9$ phase had not significant effect on τ_f values of MN

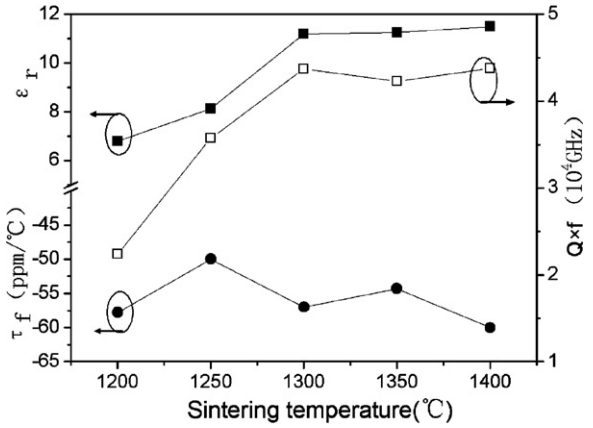

Fig. 7. Curves of ε_r, $Q{\cdot}f$ and τ_f values of MN ceramics in the temperature region of 1200–1400 °C as a function of sintering temperatures.

ceramics due to approximate τ_f value of −54 ppm/°C [14,15]. As we known, τ_f value of dielectric ceramics as an intrinsic parameter independent of fabrication process was associated with the temperature coefficient of dielectric constant (τ_ε) and thermal expansion coefficient (α_L). Thus, it was considered that additional improvement in τ_f values was required for dielectric resonator applications at high frequency.

4. Conclusions

The aqueous sol–gel route was used to synthesize pseudobrookite-type structure $Mg_5Nb_4O_{15}$ powders with particle sizes of nearly 20–40 nm, which showed major advantages over conventional solid-state methods reported before. A considerable decrease in calcination temperature (at 600 °C) was obtained in pure oxygen atmosphere for the formation of $Mg_5Nb_4O_{15}$ nanopowders. Moreover, the sintering ability and microwave properties of $Mg_5Nb_4O_{15}$ ceramics were systematically investigated with the increase of sintering temperature. The $Mg_5Nb_4O_{15}$ sample with nearly full density was obtained at 1300 °C and showed excellent microwave dielectric properties of ε_r ∼11.3, $Q{\cdot}f$ ∼43,300 GHz and τ_f ∼−58 ppm/°C. Experimental results showed that the aqueous sol–gel process was of high efficiency to synthesize nanosized powders with larger surface area and high free energy, which was beneficial to reduce sintering temperatures and optimize $Mg_5Nb_4O_{15}$ ceramics' performance.

Acknowledgements

This work was supported by the Natural Science Youth Foundation of Shandong Province (No. ZR2011EMQ005) and the National Natural Science Foundation (No. 51172093, 51042009).

References

[1] I.N. Jawahar, P. Mohanan, M.T. Sebastian, $A_5B_4O_{15}$ (A = Ba, Sr, Mg, Ca, Zn; B = Nb, Ta) microwave dielectric ceramics, Mater. Lett. 57 (2003) 4043–4048.
[2] S. Pagola, R.E. Carbonio, M.T. Fernandez-Diaz, J.A. Alonso, Crystal structure refinement of $Mg_5Nb_4O_{15}$ and $Mg_5Ta_4O_{15}$ by Rietveld analysis of neutron powder diffraction data, J. Solid State Chem. 137 (1998) 359–364.
[3] S. Kamba, J. Petzelt, E. Buixaderas, D. Haubrich, P. Vaněk, High frequency dielectric properties of $A_5B_4O_{15}$ microwave ceramics, J. Appl. Phys. 89 (2001) 3900–3906.
[4] H.S. Zhu, Z.J. Guo, W.D. Yang, W.F. Chang, C.C. Wang, Preparation and characterization of nanometer-sized $(Pb_{1-x}Ba_x)TiO_3$ powders using acetylacetone as a chelating agent in a non-aqueous sol–gel process, Ceram. Int. 37 (2011) 3203–3209.
[5] N.L. Wang, X.Y. Zhang, Z.H. Bai, H.Y. Sun, Q.S. Liu, L.P. Lu, X.Y. Mi, X.C. Wang, Synthesis of nanocrystalline ytterbium-doped yttria by citrate-gel combustion method and fabrication of ceramic materials, Ceram. Int. 37 (2011) 3133–3138.
[6] M.J.N. Isfahani, P.N. Isfahani, K.L.D. Silva, A. Feldhoff, Structural and magnetic properties of $NiFe_{2-x}Bi_xO_4$ ($x = 0$, 0.1, 0.15) nanoparticles prepared via sol–gel method, Ceram. Int. 37 (2011) 1905–1909.
[7] A.K. Zak, W.H. Abd Majid, Effect of solvent on structure and optical properties of PZT nanoparticles prepared by sol–gel method, in infrared region, Ceram. Int. 37 (2011) 753–758.
[8] M.H. Ardakani, F. Moztarzadeh, M. Rabiee, A.R. Talebi, Synthesis and characterization of nanocrystalline merwinite ($Ca_3Mg(SiO_4)_2$) via sol–gel method, Ceram. Int. 37 (2011) 175–180.
[9] B.W. Hakki, P.D. Coleman, A dielectric resonator method of measuring inductive capacities in the millimeter range, IEEE Trans. 8 (1960) 402–410.
[10] W.E. Courtney, Analysis and evaluation of a method of measuring the complex permittivity and permeability of microwave insulators, IEEE Trans. 18 (1970) 476–485.
[11] Y.K. Lakshmi, P.V. Reddy, Influence of sintering temperature and oxygen stoichiometry on electrical transport properties of $La_{0.67}Na_{0.33}MnO_3$ manganite, J. Alloys Compd. 470 (2009) 67–74.
[12] A. Thorvaldsen, The intercept method. 2. Determination of spatial grain size, Acta Mater. 45 (1997) 595–600.
[13] S.-J.L. Kang, Sintering: Densification, Grain Growth & Microstructure, Elsevier Butterworth-Heinemann, Burlington, 2005.
[14] H. Ogawa, A. Kan, S. Ishihara, Y. Higashida, Crystal structure of corundum type $Mg_4(Nb_{2-x}Ta_x)O_9$ microwave dielectric ceramics with low dielectric loss, J. Eur. Ceram. Soc. 23 (2003) 2485–2488.
[15] L.A. Khalam, S. Thomas, M.T. Sebastian, Tailoring the microwave dielectric properties of $MgNb_2O_6$ and $Mg_4Nb_2O_9$ ceramics, Int. J. Appl. Ceram. Technol. 4 (2007) 359–366.
[16] R.D.S. Shannon, G.R. Rossman, Dielectric constants of silicate garnets and the oxide additivity rule, Am. Miner. 77 (1992) 94–100.
[17] R.D.S. Shannon, Dielectric polarizabilities of ions in oxides and fluorides, J. Appl. Phys. 73 (1993) 348–366.
[18] S.J.S. Penn, M.N. Alford, A. Templeton, X. Wang, M. Xu, M. Reece, K. Schrapel, Effect of porosity and grain size on the microwave dielectric properties of sintered alumina, J. Am. Ceram. Soc. 80 (1997) 1885–1888.
[19] K. Sreedhar, N.R. Pavaskar, Synthesis of $MgTiO_3$ and $Mg_4Nb_2O_9$ using stoichiometrically excess MgO, Mater. Lett. 53 (2002) 452–455.
[20] Z.F. Fu, P. Liu, X.M. Chen, J.L. Ma, H.W. Zhang, Low-temperature synthesis of $Mg_4Nb_2O_9$ nanopowders by high-energy ball-milling method, J. Alloys Compd. 493 (2010) 441–444.
[21] W.D. Kingery, Introduction to Ceramics, 2nd ed., Wiley, New York, 1976.